Spectroscopic analyses of Manganase ions effects of conformational changes of Sh-PPase

by Elvy Like Ginting 30

Submission date: 01-Mar-2021 04:04PM (UTC-0800)
Submission ID: 1521753129
File name: Manganase_ions_effects_of_conformational_changes_of_Sh-PPase.pdf (679.22K)
Word count: 4655
Character count: 25173

Spectroscopic Analyses of Manganese Ions Effects on the Conformational Changes of Inorganic Pyrophosphatase from Psychrophilic Shewanella *sp. AS-11*

Elvy Like Ginting, Chihiro Maeganeku, Hiroyuki Motoshima & Keiichi Watanabe

The Protein Journal

ISSN 1572-3887
Volume 33
Number 1

Protein J (2014) 33:11-17
DOI 10.1007/s10930-013-9531-0

Springer

Protein J (2014) 33:11–17
DOI 10.1007/s10930-013-9531-0

Spectroscopic Analyses of Manganese Ions Effects on the Conformational Changes of Inorganic Pyrophosphatase from Psychrophilic *Shewanella* sp. AS-11

Elvy Like Ginting · Chihiro Maeganeku · Hiroyuki Motoshima · Keiichi Watanabe

Published online: 21 December 2013

Abstract Mn^{2+} ions influence the activity, temperature dependence, and thermostability of the psychrophilic *Shewanella*-PPase (*Sh*-PPase), and are required to function in cold environments. The functional characteristics of *Sh*-PPase on activation with Mn^{2+} ions are possibly related to conformational changes in the molecule. In this study, conformational changes of *Sh*-PPase on activation with Mn^{2+} ions were analyzed in solution by fluorescence spectroscopy analysis of intrinsic tryptophan residues, 1-anilino-8-naphthalene sulfonate fluorescence, and circular dichroism spectroscopy. For *Sh*-PPase, Mn^{2+} ions did not affect the flexibility of the tryptophan residues and secondary structure of the enzyme. However, the microenvironment of the tryptophan residues and surface area of *Sh*-PPase were more hydrophilic on activation with Mn^{2+} ions. These results indicate that activation with Mn^{2+} ions causes conformational changes around the aromatic amino acid residues and affects the hydrophobicity of the enzyme surface, which results in conformational changes. Substrate-induced conformational changes reflect that metal-free *Sh*-PPase in solution indicated an open structure and will be a close structure when binding substrate. In combination of our spectroscopic analyses on *Sh*-PPase, it can be concluded that activation with Mn^{2+} ions changes some conformation of *Sh*-PPase molecule in solution.

Keywords Conformational changes · Inorganic pyrophosphatase · Manganese ions · Spectroscopy

Abbreviations

ANS	1-Anilino-8-naphthalene sulfonate
Bs-PPase	Inorganic pyrophosphatase from *Bacillus subtilis*
CD	Circular dichroism
EDTA	Ethylenediamine-*N*,*N*,*N*′,*N*′-tetraacetic acid
Ec-PPase	Inorganic pyrophosphatase from *Escherichia coli*
Sg-PPase	Inorganic pyrophosphatase from *Streptococcus gordonii*
Sh-PPase	Inorganic pyrophosphatase from psychrophilic *Shewanella* sp. AS-11
Trp	Tryptophan

1 Introduction

Inorganic pyrophosphatase (PPase) is an enzyme that catalyzes the hydrolysis of inorganic pyrophosphate into two phosphates [1]. This is essential for all living organisms, and has also been demonstrated in bacteria [2] and yeast [3]. The two soluble PPase families that have been found were I and II which different fully in their primary structures. Homodimer family I PPases are found in eukaryotes, whilst those found in prokaryotes are homohexamer with both having one-domain subunits [4]. While the family I PPases are found in all living organisms, the family II PPases can only be found in archaebacteria and bacteria [5, 6]. A homodimer structure was found in family II PPases

E. L. Ginting (✉) · C. Maeganeku · H. Motoshima · K. Watanabe (✉)
Department of Applied Biochemistry and Food Science, Saga University, 1-Honjo-machi, Saga 840-8502, Japan
e-mail: sn9073@edu.cc.saga-u.ac.jp

K. Watanabe
e-mail: watakei@cc.saga-u.ac.jp

E. L. Ginting · K. Watanabe
The United Graduate School of Agricultural Sciences, Kagoshima University, Kagoshima, Japan

that have two-domain subunits (the N- and C-domains) [7, 8]. These two domains are connected flexibly with a hinge, and the active site is situated between these domains [5].

Both families of PPases are only active in the presence of metal ion cofactors, which are involved in physiological hydrolysis of inorganic pyrophosphate but differ in their catalytic properties and structures. Family I PPases show strong metal ion dependency, with Mg^{2+} ions providing the highest inorganic pyrophosphate-hydrolyzing activity [9]. Family II PPases are more active with Mn^{2+} or Co^{2+} ions than Mg^{2+} ions [6]. The activity of family II PPases is 20 times higher with Mn^{2+} ions than with Mg^{2+} ions [10].

In an earlier study, PPase from *Shewanella* sp. AS-11 (*Sh*-PPase) was successfully cloned as (DDBJ/EMBL/GenBank, accession number: AB775531) and expressed in *Escherichia coli*. *Sh*-PPase was found to be a family II PPase. The molecular mass of *Sh*-PPase was 34 kDa [11]. *Shewanella* sp. AS-11 is a psychrophilic bacterium that can be isolated from shellfish living in the Antarctic ice-covered sea where temperatures are close to and often below 0 °C. Compared with enzymes from mesophilic bacteria, the homologues enzymes from psychrophilic bacteria generally have higher activities at low temperatures [12] and lower thermostability. Preliminary studies on *Sh*-PPase have shown that its activity, temperature dependence, and thermostability are greatly influenced by Mn^{2+} ions. Furthermore, Mn^{2+} ions are required for the cold-adaption of *Sh*-PPase [11]. These functional characteristics of *Sh*-PPase on activation with Mn^{2+} ions are possibly related to conformational changes of the enzyme. Therefore, it is essential to study the conformational changes of inorganic pyrophosphatase from the psychrophilic *Shewanella* sp. on activation with Mn^{2+}.

In this study, the conformation of *Sh*-PPase upon activation with Mn^{2+} was analyzed using spectroscopic methods. In order to find the conformational changes of the protein, the intrinsic fluorescence spectra of tryptophan residues was used as a useful tool because of its extreme sensitivity to the local environment [13–16]. In addition, to detect the structure of the protein, a quenching of fluorescence was also commonly used [16–18]. *Sh*-PPase has two tryptophan residues per monomer (Trp109 and Trp286). These two residues were used as an intrinsic fluorescence probe and the acrylamide as quencher to monitor enzyme conformational changes. 1-Anilino-8-naphthalene sulfonate (ANS) was used as an extrinsic fluorescent probe to analyze the changes in the structure of the ANS binding site of the enzyme. This probe binds to hydrophobic sites in proteins and is extremely sensitive to the polarity of its environments [13, 19]. The secondary structure of *Sh*-PPase was examined by using circular dichroism (CD) spectra [20].

2 Materials and Methods

2.1 Expression and Purification

The recombinant *Sh*-PPase was expressed in *E. coli* BL21 (DE3) at 20 °C using pET16b as an expression vector and purified from the cell extracts by a combination of ammonium sulfate fractionation and anion-exchange chromatography using a Hi-Trap Q HP column (GE Healthcare Bio-Sciences, Sweden), as described in [11]. The protein concentrations were determined by the Bradford method [21] using the protein dye reagent (Bio-Rad Laboratories, Life Science Group, Hercules, CA) and bovine serum albumin as the standard.

2.2 Preparation of Metal-Free and Mn-Activated *Sh*-PPases

Metal-free (non-activated) *Sh*-PPase was prepared by Ethylenediamine-*N*,*N*,*N*′,*N*′-tetraacetic acid (EDTA) treatment of the enzyme followed by ultra filtration on Amicon ultra centrifugal filter devices (30-kDa cutoff). The enzyme solution (10 mg/mL) was diluted 50-fold with 100 mmol/L Tris/HCl buffer (pH 7.5) containing 2 mmol/L EDTA and 50 mmol/L KCl, and subjected to ultra filtration. The enzyme was then diluted 50-fold again with 100 mmol/L Tris/HCl buffer (pH 7.5) containing 20 µmol/L EDTA and 50 mmol/L KCl and subjected to two dilution/concentration cycles by using ultra filtration. The final solution was adjusted to 3–5 mg/mL enzyme and stored at −80 °C.

Mn-activated *Sh*-PPase was prepared by incubating the metal-free enzyme for 2 h at 5 °C with 15 mmol/L $MnCl_2$ in 100 mmol/L Tris/HCl buffer (pH 7.5) containing 20 µmol/L EDTA and 50 mmol/L KCl. The activated enzymes containing Mn^{2+} ions in the active sites were prepared by three dilution/concentration cycles with the same buffer but containing 40 µmol/L $MnCl_2$ using ultra filtration on Amicon ultra centrifugal filter devices. The Mn-activated *Sh*-PPase contained two Mn atoms per monomer as determined by inductively coupled plasma-atomic emission spectroscopy (ICP-AES), while no Mn atom was detected in the metal-free *Sh*-PPase [11].

2.3 Fluorescence Spectroscopy

Fluorescence spectra were recorded on a Hitachi 850 fluorescence spectrophotometer. Each spectrum was averaged from three scans. The excitation wavelength was set at 295 nm to preferentially excite the two tryptophan residues per monomer rather than tyrosine residues. The non-activated and Mn-activated *Sh*-PPase samples (0.1 mg/mL) were prepared in 100 mmol/L Tris–HCl buffer (pH 7.5) containing 50 mmol/L KCl and 20 µmol/L EDTA. The

Mn-activated *Sh*-PPase sample also contained 40 µmol/L $MnCl_2$. The fluorescence spectra on non-activated and Mn-activated *Sh*-PPases for substrate induced conformational changes; enzyme contained 1 mmol/L imidodiphosphate (PNP). The emission spectra were recorded at 25 °C between 310 and 400 nm with 5-nm excitation and emission band passes.

In fluorescence quenching experiments, acrylamide was added to the samples and the fluorescence spectra were recorded. The final quencher concentration in each sample was 400 mmol/L. Steady-state fluorescence quenching data were analyzed by the following Stern–Volmer equation to obtain quantitative quenching parameters [13]:

$$F_o/F = 1 + K_{sv}[Q],$$

where F_o and F are the relative fluorescence intensities in the absence and presence of the quencher, respectively; $[Q]$ is the quencher concentration; and K_{sv} is Stern–Volmer quenching constant. The values of K_{sv} with different samples were obtained from the slopes of plots of F_o/F versus $[Q]$.

Steady state fluorescence anisotropy was measured using the same instrument. After measuring the parallel (I_{vv}) and perpendicular (I_{vh}) components of emission against the vertical excitation, fluorescence anisotropy (r) was calculated using the following equation:

$$r = (I_{vv} - GI_{vh})/(I_{vv} + 2GI_{vh}),$$

where G is the grating factor, which is determined by the intensity ratio of the vertical component to the horizontal component against the horizontal excitation.

For ANS assays, the excitation wavelength was set at 380 nm while the emission was recorded between 400 and 600 nm. The concentrations of ANS and the enzyme were 50 µmol/L and 0.1 mg/mL, respectively. ANS fluorescence spectra for substrate inducing the conformational change enzyme contained 1 mmol/L PNP. All measurements were performed at 25 °C.

2.4 Circular Dichroism Spectroscopy

CD spectra were recorded at 25 °C on a Jasco spectropolarimeter (Jasco International Co., Ltd., Tokyo, Japan). Samples were placed in a rectangular quartz cell with 0.1 mm path length. The concentrations of non-activated and Mn-activated *Sh*-PPase were both 0.2 mg/mL in 20 mmol/L Tris–HCl buffer (pH 7.5) containing 50 mmol/L KCl and 20 µmol/L EDTA. The Mn-activated *Sh*-PPase also contained 40 µmol/L of the activating metal ion. Measurements were recorded at 250–700 nm. CD data were averaged from four scans. The CD spectra of the appropriate buffers were recorded and subtracted from the protein spectra. The CD data are expressed in terms of mean residue ellipticity (θ).

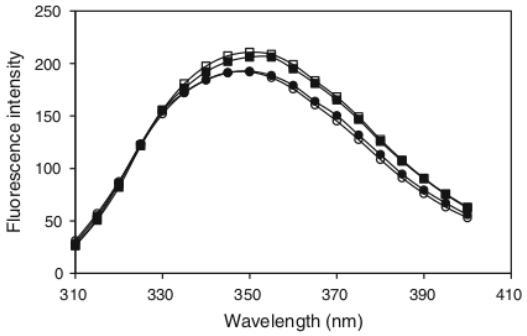

Fig. 1 The fluorescence spectra of non-activated (*circle*) and Mn-activated (*square*) *Sh*-PPases in the absence (*open symbols*) or the presence (*closed symbols*) of substrate analog PNP. The enzymes (0.2 mg/mL) in 100 mmol/L Tris–HCl buffer containing 50 mmol/L KCl and 20 µmol/L EDTA, pH 7.5 were recorded between 310 and 400 nm at an excited wavelength of 295 nm with excitation and emission band passes of 5-nm, at 25 °C. The Mn-activated sample also contained 40 µmol/L $MnCl_2$. The PNP concentration was 1 mmol/L

2.5 Construction of Molecular Model Structure

The three-dimensional (3D) model structure of *Sh*-PPase was built using a program MODELLER (http://salilab.org/modeller) [22] on the basis of the sequence homology to family II PPase from *Bacillus subtilis* as the template structure (PDB ID: 1K23, 1WPM).

3 Results

3.1 Tryptophan Fluorescence of *Sh*-PPase

The intrinsic fluorescence emission spectra of non-activated and Mn-activated *Sh*-PPases are shown in Fig. 1. The emission maxima wavelengths of non-activated and Mn-activated *Sh*-PPases were 348 and 352 nm, respectively, when excited at 295 nm. Furthermore, the fluorescence spectra of non-activated and Mn-activated *Sh*-PPases were not change-induced substrate for conformational changes.

Figure 2 shows Stern–Volmer plots of fluorescence quenching of the acrylamide of non-activated and Mn-activated *Sh*-PPases. The values of Stern–Volmer quenching constant (K_{sv}) of the non-activated *Sh*-PPase were 7.40 in the absence of the substrate and 4.62 M^{-1} with substrate-induced conformational changes. The values of K_{sv} of Mn-activated *Sh*-PPase were 4.18 in the absence of the substrate and 3.93 M^{-1} with substrate-induced conformational changes. The results indicated that fluorescence quenching of the acrylamide of Mn-activated *Sh*-PPase was lower than the non-activated *Sh*-PPase. On the other hand,

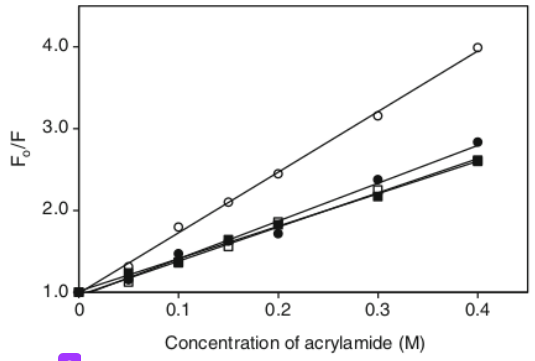

Fig. 2 Stern–Volmer plots of fluorescence quenching for acrylamide of non-activated (*circle*) and Mn-activated (*square*) *Sh*-PPases. *Sh*-PPases without substrate analog PNP are open symbols and while the substrate analog PNP are closed symbols. Fluorescence intensities of non-activated enzyme were measured at 348 nm and Mn-activated enzyme was at 352 nm. They were excited at 295 nm with various concentrations of acrylamide quenchers. All other conditions for fluorescence measurements were the same as in Fig. 1. F_o is the fluorescence intensities without acrylamide and F was the fluorescence intensities with acrylamide. The values of the K_{sv} quenching constant of the non-activated *Sh*-PPase were 7.40 in the absence of PNP and 4.62 M^{-1} in the presence of PNP. The values of the K_{sv} quenching constant of Mn-activated *Sh*-PPase were 4.18 in the absence of PNP and 3.93 M^{-1} in the presence of PNP

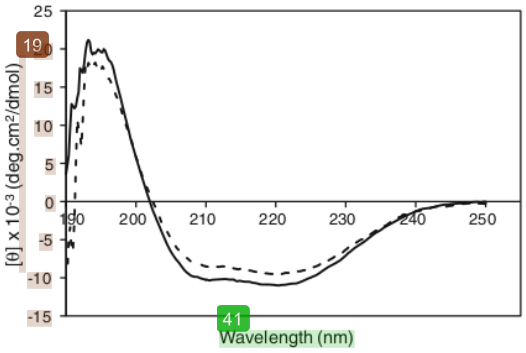

Fig. 3 The CD spectra of non-activated and activated *Sh*-PPases. The CD spectra of non-activated (*solid line*) and activated enzyme (*dashed line*) (0.2 mg/mL) were recorded at 250–190 nm at 25 °C for four scans and the averaged data was shown after subtraction of the buffer blank data

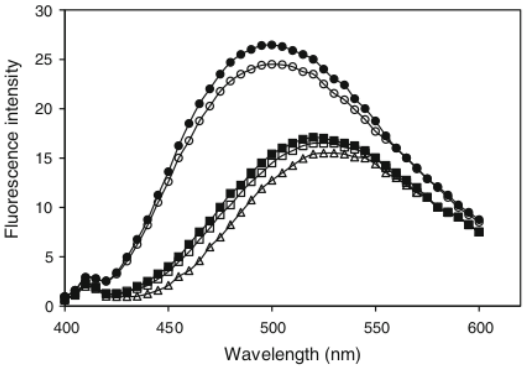

Fig. 4 The ANS (50 µmol/L) fluorescence spectra on non-activated (*open circle*) and Mn-activated (*open square*) *Sh*-PPase (0.2 mg/mL) in 100 mmol/L Tris–HCl buffer contained 50 mmol/L KCl and 20 µmol/L EDTA, pH 7.5 were recorded between 400 and 600 nm at an excited wavelength of 380 nm with excitation and emission band passes of 5-nm, at 25 °C. The ANS (50 µmol/L) fluorescence spectra on non-activated (*closed circle*) and Mn-activated (*closed square*) for substrate inducing conformational change enzymes contained 1 mmol/L PNP. Mn-activated *Sh*-PPase also contained 40 µmol/L of activated metal ion. The *open triangle* is a 50 µmol/L ANS in 100 mmol/L Tris–HCl buffer containing 50 mmol/L KCl and 20 µmol/L EDTA, pH 7.5

Stern–Volmer quenching constant of the Mn-activated *Sh*-PPase was not significantly changed although it was induced by the substrate. Based on Fig. 2 is showing that the acylamide quenching of non-activated and Mn-activated *Sh*-PPases revealed linear Stern–Volmer plots.

Fluorescence from tryptophan is known to be sensitive to the polarity or rotational motion of its local environment [23]. The anisotropies of non-activated and Mn-activated *Sh*-PPases were 0.117 and 0.112, respectively. The fluorescence anisotropies of tryptophan of the non-activated and Mn-activated *Sh*-PPases were similar.

3.2 Circular Dichroism Spectra of *Sh*-PPase

Figure 3 shows the CD spectra of non-activated and activated *Sh*-PPases. The CD spectra in the far ultraviolet region both of non-activated and Mn-activated *Sh*-PPases had two negative bands at 222 and 208 nm, and a positive band at ~ 190 nm all of which were typical of α-helical structure [20]. Therefore, there are no differences in secondary structures of non-activated and Mn-activated *Sh*-PPases.

3.3 Fluorescence Changes on the Binding of ANS to *Sh*-PPase

The extrinsic fluorescence results obtained using ANS as a fluorescent probe are shown in Fig. 4. The maximum emission of non-activated *Sh*-PPase bound to ANS was 500 nm and Mn-activated *Sh*-PPase bound to ANS was 520 nm, when excited at 380 nm. These results show the maximum emission of Mn-activated *Sh*-PPase bound to ANS was red shifted. Figure 4 also shows the fluorescence intensity of Mn-activated *Sh*-PPase bound to ANS was decreased compared with the non-activated *Sh*-PPase bound to ANS. This could be attributed to the hydrophobicity of the binding site and the restricted mobility of ANS

[19]. The fluorescence intensity of non-activated *Sh*-PPase bound to ANS was increased inducing a substrate for conformational changes. On the other hand, there was no change to the extrinsic fluorescence of Mn-activated *Sh*-PPase bond ANS induced substrate for conformational changes.

4 Discussion

The study of *Sh*-PPase in solution showing the intrinsic fluorescence tryptophan residues of *Sh*-PPase were affected by activation with manganese ions. The microenvironment of both Trp109 and Trp286 residues became more hydrophilic and decreased the quenching effect. These results indicate that the tryptophan residues were buried within the enzyme on activation with manganese ions but still interacted with a neighboring polar group. However, being buried in the tryptophan residues did not change the flexibility of these residues.

Trp109 and Trp286 residues both of non-activated and Mn-activated *Sh*-PPases are equally quenched by acrylamide [13] that is shown in the linear Stern–Volmer plots. Activation with Mn^{2+} ions decreased the quenching effect of *Sh*-PPase indicating that conformational changes with the binding of the catalytic metal ion (Mn^{2+} ions) reduced collisional quenching of the tryptophan residues in the enzyme [24].

The results of an earlier study showed relative molecular masses for non-activated and Mn-activated *Sh*-PPases of 34 and 61 kDa, respectively [11], and these values indicate that non-activated *Sh*-PPase was a monomer and Mn-activated *Sh*-PPase was a homodimer. The conformations of non-activated and Mn-activated *Sh*-PPases showed that dimerization of the enzyme occurred, which changed the environment around the tryptophan residues. These results are consistent with those of other studies, and suggest that binding divalent cations to thermophilic PPase causes conformational changes around the aromatic amino acid residues and leads to dimerization of the enzyme [25].

On the other hand, no change in the secondary structures of the enzyme was found, indicating that the conformational change may be rather subtle, e.g., a change in the state of aromatic acid residues as detected by the fluorescence spectra. These results are similar to earlier results that showed the secondary structure of thermophilic PPase was not changed on the addition of divalent cations [25] and the polypeptide backbone of *Escherichia coli*-PPase (*Ec*-PPase) was unaltered by chemical modification [26].

The results of extrinsic fluorescence using an ANS probe also showed the conformational changes of *Sh*-PPase on activation with Mn^{2+} ions. Activation with Mn^{2+} ions caused the surface of *Sh*-PPase to become hydrophilic compared to non-activated *Sh*-PPase that showed increased solvent polarity. Increased solvent polarity will generally decrease the fluorescence intensity and cause a red shift in the λ_{max} of emission [15]. These results also reveal that dimerization changed the hydrophobic surface of this enzyme. While the surface of the *Sh*-PPase monomer was hydrophobic, two monomers packed together on dimerization. This concealed the hydrophobic surfaces and made the homodimer surface hydrophilic.

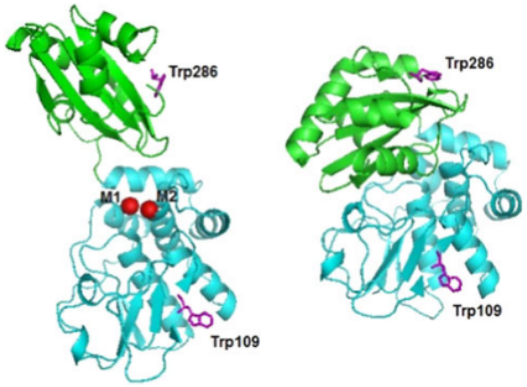

Fig. 5 Model structures of open (*left*) and closed (*right*) *Sh*-PPases. The open and closed structures were built using the known structures of PPase from *Bacillus subtilis* as templates (PDB ID: 1K23 and 1WPM, respectively). The N-domain is shown in *cyan* and C-domain including the interdomain hinge region shown in *green*. Two metal ions (M1 and M2 shown as *red spheres*) are located at the positions corresponding to those of Mn^{2+} bound to *B. subtilis* enzyme. Trp109 and Trp286 are shown as sticks (*magenta*). The diagrams were prepared using PyMOL (Color figure online)

A three-dimensional model of *Sh*-PPase was built using a program MODELLER to determine the positions of the tryptophan residues in the *Sh*-PPase. The model was based on the known structure of the mesophilic PPase from *Bacillus subtilis* (*Bs*-PPase) (PDB ID: 1K23 for open structure and 1WPM for closed structure) (Fig. 5). The amino acid sequence of *Sh*-PPase has a 36.69 % identity with *Bs*-PPase. The model structure of *Sh*-PPase is showing that the two tryptophan residues per monomer are Trp109 and Trp286, and the two manganese ions are M1 and M2. The manganese ion-binding site (M1) was 24 Å from Cα of Trp109 and 23 Å from Cα of Trp286, but activation with manganese ions modified residues in the environment surrounding the tryptophan residues. This suggests that the conformation of the *Sh*-PPase molecule could be changed upon activation with manganese ions providing details about the dynamics [17] of *Sh*-PPase.

The structures of family II PPases (*Bs*-PPase*Mn core, *S. gordonii*-PPase*Zn (*Sg*-PPase) and *Bs*-PPase) from X-ray crystallography revealed that all of these structures are similar [7, 8, 27] on bound metal ions or metal-free

structures. But, these results of the structure of *Sh*-PPase in solution clearly show the conformational change of the enzyme on the binding metal ion.

The family II PPases are homodimers of two-domain subunits (the N- and C-domains) [7, 8] that are linked by a flexible hinge. The enzyme active site is located at the interface between the N- and C-domains [5], which are substrate bound at the active site. Movement of the C-domain over the N-domain creates a catalytically competent structure [7, 8] which indicates the open and closed structure of PPase. Therefore, the interesting point is the open and closed structure of *Sh*-PPase in solution. In this regard, the substrate-induced conformational changes are observed. The intrinsic fluorescence emission maxima of the substrate bound non-activated *Sh*-PPase was not changed compared to the free substrate. However, the K_{sv} value was decreased by acrylamide quenching of the substrate-bound non-activated *Sh*-PPase. It shows that both tryptophan residues would be buried when substrate bound indicated conformational changes. The conformational changes caused by the substrate-bound non-activated *Sh*-PPase denoted the open-closed structure of *Sh*-PPase. Substrate binding induces a conformational change on the closed form, as represented by the *Sg*-PPase structure [8]. The 3D structure of *Bs*-PPase bound sulfate (PDB; 1WPM) shows a closed structure on the metal-free [27]. On the other hand, the non-activated *Sh*-PPase that did not bind the substrate indicated an open structure. The conformational changes of the non-activated *Sh*-PPase by substrate-induced conformational changes resemble Mn-activated *Sh*-PPase based on K_{sv} value. But, the intrinsic fluorescence maxima and K_{sv} of Mn-activated *Sh*-PPase were not changed although they were induced by a substrate. It shows that Mn-activated *Sh*-PPase is still a closed structure in solution. The structure of family II PPases (*Bs*-PPase and *Sg*-PPase) [27] showed sulfate binding to the C-domain which is correlated with the closed conformation on binding metal ions.

The conformational changes of non-activated *Sh*-PPase by an induced substrate is supported by the results of extrinsic fluorescence obtained using ANS as a fluorescence probe. These results revealed that bound-substrate changed the surface area of non-activated *Sh*-PPase bound ANS. On the other hand, bound-substrate did not change the surface area of Mn-activated *Sh*-PPase bound ANS. It could also indicate that the conformational changes from opened structure to closed structure of non-activated *Sh*-PPase are induced by substrate.

In conclusion, activation with Mn^{2+} ions caused some conformational changes of psychrophilic *Sh*-PPase in solution and provided conformational changes/dynamics of *Sh*-PPase. Conformational changes of psychrophilic *Sh*-PPase in solution may be rather subtle, as detected by the fluorescence spectra but did not change the secondary structure. However the conformation change of *Sh*-PPase in solution on activation with Mn^{2+} ions did not delineate the functional characteristics of the *Sh*-PPase. The high activity of Mn-activated *Sh*-PPases at low temperatures (cold-adaptation) could be attributed to the flexible structure around the active center [28], or related to the flexible geometry coordination [27] of the amino acids in the PPase and the Mn^{2+} ions.

Acknowledgments We would like to thank Prof. Dr. Yoichiro Hama and Prof. Dr. Yasushi Sugano for their interest, encouragement, and valuable discussions. This study was supported by the Directorate General of Higher Education (DIKTI-Indonesia) scholarship and by the Rendai-student Supporting program of the United Graduate School of Agricultural Sciences, Kagoshima University to ELG.

Conflict of interest The authors declare that they have no conflict of interest.

References

1. Baykov AA, Cooperman BS, Lahti R (1999) In: Schroder (ed) Cytoplasmic inorganic pyrophosphatase. Springer, Berlin
2. Chen J, Brevet A, Fromant M, Leveque F, Schmitter J-M, Blanquet S, Plateau P (1990) J Bacteriol 172:5686–5689
3. Lundin M, Baltscheffsky H, Ronne H (1991) J Biol Chem 266:12168–12172
4. Zyryanov AB, Vener AV, Salminen A, Goldman A, Lahti R, Baykov AA (2004) Biochemistry 43:1065–1074
5. Young TW, Kuhn NJ, Wadeson A, Ward S, Burges D, Cooke GD (1998) Microbiology 144:2563–2571
6. Shintani T, Uchiumi T, Yonezawa T, Salminen A, Baykov AA, Lahti R, Hachimori A (1998) FEBS Lett 439:263–266
7. Merckel MC, Fabrichniy IP, Salminen A, Kalkkinen N, Baykov AA, Lahti R, Goldman A (2001) Structure 9:289–297
8. Ahn S, Milner AJ, Futterer K, Konopka M, Ilias M, Young TW, White SA (2001) J Mol Biol 313:797–811
9. Islam MK, Miyoshi T, Isobe T, Kasuga-Aoki H, Arakawa T, Matsumoto Y, Yokomizo Y, Tsuji N (2004) J Vet Med Sci 66:221–223
10. Perfenyev AN, Salminen A, Halonen P, Hachimori A, Baykov AA, Lahti R (2001) J Biol Chem 276:24511–24518
11. Ginting EL, Iwasaki S, Maeganeku C, Motoshima H, Watanabe K (2013) Prep Biochem Biotech (in press)
12. Morita RY (1975) Bacteriol Rev 39:144–167
13. Lakowicz JR (2006) Principles of fluorescence spectroscopy, 3rd edn. Springer, Singapore
14. Eftink MR (2000) In: Lakowicz JR (ed) Intrinsic fluorescence of protein, topics in fluorescence spectroscopy, vol 6: protein fluorescence. Kluwer Academic/Plenum, New York
15. Moller M, Denicola A (2002) Biochem Mol Biol Educ 30:309–312
16. Tang MAK, Motoshima H, Watanabe K (2012) Protein J 31:337–344
17. Chang G-G, Lee H-J (1984) J Biochem Biophys Methods 9:351–355
18. Eftink MR, Ghiron CA (1987) Biochim Biophys Acta 916:343–349
19. Gasymov OK, Glasgow B (2007) J Biochim Biophys Acta 1774:403–411

20. Manavalan P, Johnson WCJJR (1985) Proc Int Symp Biomol Struct Interact Suppl J Biosci 8:141–149
21. Bradford MM (1976) Anal Biochem 72:248–254
22. Sali A, Blundell TL (1993) J Mol Biol 234:779–815
23. Vivian JT, Callis PR (2001) Biophys J 80:2093–2109
24. Brewer JM, Bastiaens P, Lee J (1987) Biochem Biophys Res Commun 147:329–334
25. Hachimori A, Shiroya Y, Hirato A, Miyahara T, Samejima T (1979) J Biochem 86:121–130
26. Kaneko S-I, Ichiba T, Hirano N, Hachimori A (1993) Int J Biochem 25:233–238
27. Fabrichniy IP, Lehtio L, Salminen A, Zyryanov AB, Baykov AA, Lahti R, Golman A (2004) Biochemistry 43:14403–14411
28. Feller G, Narinx E, Aprigny JL, Aittaleb M, Baise E, Genicot S, Gerday C (1989) FEMS Microbiol Rev 18:189–202

Spectroscopic analyses of Manganase ions effects of conformational changes of Sh-PPase

ORIGINALITY REPORT

16%	11%	14%	4%
SIMILARITY INDEX	INTERNET SOURCES	PUBLICATIONS	STUDENT PAPERS

PRIMARY SOURCES

1	fqb.fcien.edu.uy Internet Source	1%
2	bloodjournal.hematologylibrary.org Internet Source	1%
3	Charlotte Lan. "Structural and dynamic properties of juxta-membrane segments of caveolin-1 and caveolin-2 at the membrane interface", European Biophysics Journal, 10/22/2009 Publication	1%
4	Biswas, Ashis, Antonia Miller, Tomoko Oya-Ito, Puttur Santhoshkumar, Manjunatha Bhat, and Ram H. Nagaraj. "Effect of Site-Directed Mutagenesis of Methylglyoxal-Modifiable Arginine Residues on the Structure and Chaperone Function of Human αA-Crystallin†", Biochemistry, 2006. Publication	1%
5	mafiadoc.com	

	Internet Source	1%
6	www.thieme-connect.com Internet Source	1%
7	doi.crossref.org Internet Source	<1%
8	Bose, D.. "Binding of a cationic phenazinium dye in anionic liposomal membrane: a spectacular modification in the photophysics", Chemistry and Physics of Lipids, 201001 Publication	<1%
9	Sandra Rocha. "The conformation of fusogenic B18 peptide in surfactant solutions", Journal of Peptide Science, 04/2008 Publication	<1%
10	jb.asm.org Internet Source	<1%
11	Hoe, H.S.. "Expression in Escherichia coli of the Thermostable Inorganic Pyrophosphatase from the Aquifex aeolicus and Purification and Characterization of the Recombinant Enzyme", Protein Expression and Purification, 200111 Publication	<1%
12	www.chemistry.ucsc.edu Internet Source	<1%

13	etd.fcla.edu Internet Source	<1%
14	Joanna Pawlat, Nobuya Hayashi, Chobei Yamabe, Iwo Pollo. "Generation of Oxidants with a Foaming System and its Electrical Properties", Ozone: Science & Engineering, 2002 Publication	<1%
15	Ahn, S.. "The "open" and "closed" structures of the type-C inorganic pyrophosphatases from Bacillus subtilis and Streptococcus gordonii", Journal of Molecular Biology, 20011102 Publication	<1%
16	Pasi Halonen, Marko Tammenkoski, Laila Niiranen, Sauli Huopalahti et al. " Effects of Active Site Mutations on the Metal Binding Affinity, Catalytic Competence, and Stability of the Family II Pyrophosphatase from ", Biochemistry, 2005 Publication	<1%
17	Nabil A. M. Sultan. "Thermodynamic analysis of porphyrin binding to Momordica charantia (bitter gourd) lectin", European Journal of Biochemistry, 8/2004 Publication	<1%
18	es.scribd.com Internet Source	<1%

19	Gururaja, T.L.. "A novel artificial loop scaffold for the noncovalent constraint of peptides", Chemistry & Biology, 20000701 Publication	<1%
20	Yun-Li Wu, Fei He, Xi-Wen He, Wen-You Li, Yu-Kui Zhang. "Spectroscopic studies on the interaction between CdTe nanoparticles and lysozyme", Spectrochimica Acta Part A: Molecular and Biomolecular Spectroscopy, 2008 Publication	<1%
21	www.doria.fi Internet Source	<1%
22	E. Nishimoto. "Thermal Unfolding Process of Dihydrolipoamide Dehydrogenase Studied by Fluorescence Spectroscopy", Journal of Biochemistry, 08/05/2006 Publication	<1%
23	R. H. Nagaraj. "Chemical Modulation of the Chaperone Function of Human A-Crystallin", Journal of Biochemistry, 02/13/2008 Publication	<1%
24	M. Khyrul Islam. "Inorganic pyrophosphatase in the roundworm Ascaris and its role in the development and molting process of the larval stage parasites", European Journal of Biochemistry, 7/2003 Publication	<1%

25	s3.amazonaws.com Internet Source	<1%
26	Rubina Mushtaq, Abdul Shakoori, Juan Jurat-Fuentes. "Domain III of Cry1Ac Is Critical to Binding and Toxicity against Soybean Looper (Chrysodeixis includens) but Not to Velvetbean Caterpillar (Anticarsia gemmatalis)", Toxins, 2018 Publication	<1%
27	Shivesh Kumar, Ejaz Ahmad, M. Shahid Mansuri, Sanjeev Kumar, Ruchi Jain, Rizwan Hasan Khan, S. Gourinath. "Crystal Structure and Trimer-Monomer Transition of N-Terminal Domain of EhCaBP1 from Entamoeba histolytica", Biophysical Journal, 2010 Publication	<1%
28	protein.bio.msu.ru Internet Source	<1%
29	www.biochemj.org Internet Source	<1%
30	www.vetres.org Internet Source	<1%
31	www.embopress.org Internet Source	<1%
32	Fujiwara-Arasaki, T.. "C-phycocyanin from a red	

	alga, Porphyra tenera: subunit structure", Biochimica et Biophysica Acta (BBA)/Protein Structure and Molecular Enzymology, 19850429 Publication	<1%
33	ubm.opus.hbz-nrw.de Internet Source	<1%
34	www.ysbl.york.ac.uk Internet Source	<1%
35	Ryung Hyo Kim, Ji Eun Park, Jeen-Woo Park. " Ceruloplasmin enhances DNA damage induced by hydrogen peroxide ", Free Radical Research, 2009 Publication	<1%
36	Submitted to Susquehanna University Student Paper	<1%
37	Boruah, Bornali, Palash M. Saikia, and Robin K. Dutta. "Binding and stabilization of curcumin by mixed chitosanâ€“surfactant systems: A spectroscopic study", Journal of Photochemistry and Photobiology A Chemistry, 2012. Publication	<1%
38	www.paper.edu.cn Internet Source	<1%
39	tel.archives-ouvertes.fr Internet Source	<1%

40	Tuominen, V.. "The R78K and D117E active-site variants of Saccharomyces cerevisiae soluble inorganic pyrophosphatase: structural studies and mechanistic implications", Journal of Molecular Biology, 19981218 Publication	<1%
41	www.j3.jstage.jst.go.jp Internet Source	<1%
42	Malgorzata E. Sztolsztener, Agnieszka Dobrzyn, Slawomir Pikula, Anna Tylki-Szymanska, Joanna Bandorowicz-Pikula. "Impaired dynamics of the late endosome/lysosome compartment in human Niemann–Pick type C skin fibroblasts carrying mutation in NPC1 gene", Molecular BioSystems, 2012 Publication	<1%
43	www.omicsonline.org Internet Source	<1%
44	Maren Vogel, Manuel Diez, Jochen Eisfeld, Michael Nassal. "In vitro assembly of mosaic hepatitis B virus capsid-like particles (CLPs): Rescue into CLPs of assembly-deficient core protein fusions and FRET-suited CLPs", FEBS Letters, 2005 Publication	<1%
45	Yuting Hu, Guowen Zhang, Jiakai Yan.	<1%

"Detection of interaction between lysionotin and bovine serum albumin using spectroscopic techniques combined with molecular modeling", Molecular Biology Reports, 2014
Publication

46	"第56回年会予稿集", Seibutsu Butsuri, 2018 Publication	<1%
47	www.researchgate.net Internet Source	<1%
48	portal.dl.saga-u.ac.jp Internet Source	<1%
49	Calabro, M.L.. "The rutin/@b-cyclodextrin interactions in fully aqueous solution: spectroscopic studies and biological assays", Journal of Pharmaceutical and Biomedical Analysis, 20050104 Publication	<1%
50	Irina N. Gorshkova, Xiaohu Mei, David Atkinson. "Arginine 123 of apolipoprotein A-I is essential for lecithin:cholesterol acyltransferase activity", Journal of Lipid Research, 2018 Publication	<1%
51	Marko Tammenkoski, Stefano Benini, Natalia N. Magretova, Alexander A. Baykov, Reijo Lahti. " An Unusual, His-dependent Family I Pyrophosphatase from ", Journal of Biological	<1%

Chemistry, 2005
Publication

52	Alexey N. Parfenyev, Anu Salminen, Pasi Halonen, Akira Hachimori, Alexander A. Baykov, Reijo Lahti. " Quaternary Structure and Metal Ion Requirement of Family II Pyrophosphatases from , , and ", Journal of Biological Chemistry, 2001 Publication	<1%

Exclude quotes	On	Exclude matches	Off
Exclude bibliography	On		